DOI: 10.1002/chem.200500236

Silver Complexes of Cyclic Hexachlorotriphosphazene

Marcin Gonsior,[a] Sasa Antonijevic,*[b] and Ingo Krossing*[b]

Abstract: The first solid-state structures of complexed $P_3N_3X_6$ (X = halogen) are reported for X = Cl. The compounds were obtained from $P_3N_3Cl_6$ and $Ag[Al(OR)_4]$ salts in CH_2Cl_2/CS_2 solution. The very weakly coordinating anion with $R = C(CF_3)_3$ led to the salt $Ag(P_3N_3Cl_6)_2^+[Al(OR)_4]^-$ (**1**), but the more strongly coordinating anion with $R' = C(CH_3)(CF_3)_2$ gave the molecular adduct $(P_3N_3Cl_6)AgAl(OR')_4$ (**3**). Crystals of $[Ag(CH_2Cl_2)(P_3N_3Cl_6)_2]^+[Al(OR)_4]^-$ (**2**), in which Ag^+ is coordinated by two phosphazene and one CH_2Cl_2 ligands, were isolated from CH_2Cl_2 solution. The three compounds were characterized by their X-ray structures, and **1** and **3** also by NMR and vibrational spectroscopy. Solution and solid-state ^{31}P NMR investigations in combination with quantum chemically calculated chemical shifts show that the ^{31}P NMR shifts of free and silver-coordinated $P_3N_3Cl_6$ differ by less than 3 ppm and indicate a very weakly bound $P_3N_3Cl_6$ ligand in **1**. The experimental silver ion affinity (SIA) of the phosphazene ligand was derived from the solid-state structure of **3**. The SIA shows that $(PNCl_2)_3$ is only a slightly stronger Lewis base than P_4 and CH_2Cl_2, while other ligands such as S_8, P_4S_3, toluene, and $1,2\text{-}Cl_2C_2H_4$ are far stronger ligands towards the silver cation. The energetics of the complexes were assessed with inclusion of entropic, thermal, and solvation contributions (MP2/TZVPP, COSMO). The formation of the cations in **1**, **2**, and **3** was calculated to be exergonic by $\Delta_r G°(CH_2Cl_2) = -97$, -107, and $-27\ kJ\,mol^{-1}$, respectively. All prepared complexes are thermally stable; formation of $P_3N_3Cl_5^+$ and AgCl was *not* observed, even at 60 °C in an ultrasonic bath. Therefore, the formation of $P_3N_3Cl_5^+$ was investigated by quantum chemical calculations. Other possible reaction pathways that could lead to the successful preparation of $P_3N_3X_5^+$ salts were defined.

Keywords: ab initio calculations · cations · NMR spectroscopy · phosphazenes · silver · weakly coordinating anions

Introduction

Cyclic phosphazenes of the general formula $(PNY_2)_n$ ($n = 3$–7) are prominent examples of inorganic ring systems[1–4] with applications in polymer chemistry.[2,5] It is known that the $P_3N_3Y_6$ molecules (Y = alkoxy, alkyl, NH_2, NHR, NR_2, etc.) are versatile ligands for transition metals, for example, $P_3N_3(NMe_2)_4(NHCH_2CH_2NH)\cdot PdCl_2$,[6] $P_3N_3(OPh)_4(Pz)_2\cdot PdCl_2$,[6] and $P_3N_3(OPh)_4(Pz)_2\cdot Mo(CO)_3$[1] (Pz = dimethylpyrazolyl). Some covalently bound complexes in which a transition-metal fragment substitutes one or two halogen atoms in $P_3N_3X_6$ (X = halogen), are also known, for example, $[(CO)_2CpFe]P_3N_3F_4$,[7] $N_3P_3Cl_5[Cr(CO)_3Cp]$,[8] and $N_3P_3Cl_4(Cp)[Mo(CO)_3Cp]$.[8] Cyclic phosphazenes such as $P_3N_3(OC_6H_4CF_3)_4(OC_6H_4F)_2$[9] are used as additives to lubricants.[10] Simple $(PNX_2)_3$ phosphazenes (X = H, F, Cl, NH_2) were studied by DFT and ab initio calculations,[9,11–16] as well as normal coordinate analyses.[17–21] These investigations were also sparked by the special electronic structure of the phosphazene rings.[11,13,16,22,23]

In the halogen-substituted $P_3N_3X_6$ cyclophosphazenes the basicity of the ring nitrogen atom is very low. Therefore, little is known about the complexing abilities of the $P_3N_3X_6$ halophosphazenes. A few complexes with AlX_3 (X = Cl, Br) have been prepared, that is, $P_3N_3Cl_6\cdot AlBr_3$[24] and $P_3N_3Br_6\cdot AlBr_3$,[24] in which it was suggested that the Al atom is N-coordinated by the phosphazene. Complexes of $P_3N_3F_6$ with PF_5, SbF_5 (but not BF_3) were also prepared.[25,26] However, at least for SbF_5, the phosphazene ring appeared to be coordinated to the Lewis acid through the F atoms rather than through the N atoms of the ring.[26] While $P_3N_3Me_6$

[a] Dr. M. Gonsior
Universität Karlsruhe (TH)
Institut für Anorganische Chemie
Engesserstrasse Geb. 30.45, 76128 Karlsruhe (Germany)

[b] Dr. S. Antonijevic,[+] Prof. I. Krossing
École Polytechnique Fédérale de Lausanne (EPFL)
Laboratory of Inorganic and Coordination Chemistry
ISIC-BCH, 1015 Lausanne (Switzerland)
E-mail: ingo.krossing@epfl.ch

[+] MAS-NMR spectroscopy.

Supporting information for this article is available on the WWW under http://www.chemeurj.org/ or from the author.

complexes with MCl_4 (M = Ti, Sn) are readily formed, $P_3N_3Cl_6$ did not react with these Lewis acids.[27] Also $P_3N_3Cl_6{\cdot}Cr(CO)_3$,[28] supposedly with an arene-like coordination, $NiCl_2{\cdot}(P_3N_3Cl_6)$,[29] and recently $VOCl_3{\cdot}P_3N_3Cl_6$[30] were prepared. For none of the $P_3N_3X_6$ complexes is a crystal structure known. Nevertheless, Lewis acid–base complexes of hexachlorotriphosphazene are relevant, since they are thought to play a key role in the polymerization to poly(dichlorophosphazene)[2,5,11,14,31] with intermediate formation of the $P_3N_3Cl_5^+$ ion.

In this work we focused on the reaction of Ag^+ with $P_3N_3Cl_6$. Of particular interest was whether $P_3N_3Cl_6$ could form a stable complex with the silver cation or would ionize and form the $P_3N_3Cl_5^+$ cation and AgCl. In related systems in which one PCl_2 moiety in $P_3N_3Cl_6$ was exchanged by SCl[32] or S(O)Cl,[33] such ionization was successful. Here we present the crystal structures and full characterization of the silver hexachlorotriphosphazene complexes $Ag(N\text{-}P_3N_3Cl_6)_2^+$, $Ag(CH_2Cl_2)(N\text{-}P_3N_3Cl_6)_2^+$ and $Ag(N\text{-}P_3N_3Cl_6)^+$. They are stabilized by weakly coordinating fluorinated alkoxyaluminates of type $[Al(OR^F)_4]^-$ (R^F = fluorinated alkyl group). These are the first structurally characterized complexes of any halogen-substituted triphosphazene.

Results

Syntheses and NMR characterization: The complexes $Ag(P_3N_3Cl_6)_2^+[Al(OR)_4]^-$ (**1**), $Ag(CH_2Cl_2)(P_3N_3Cl_6)_2^+[Al(OR)_4]^-$ (**2**), and $Ag(P_3N_3Cl_6)^+[Al(OR')_4]^-$ (**3**) were readily prepared from commercially available hexachlorotriphosphazene and the respective $Ag[Al(OR)]_4$[34] or $Ag[Al(OR')]_4$[34] salts [$R = C(CF_3)_3$, $R' = C(CH_3)(CF_3)_2$; Eq. (1)]. No AgCl precipitation was observed under these conditions.

$$Ag[Al(OR^F)_4] + P_3N_3Cl_6 \xrightarrow[-78\,^\circ C \text{ to } +60\,^\circ C,\ \text{ultrasonic enhancement}]{CH_2Cl_2} P_3N_3Cl_5^+[Al(OR^F)_4]^- + AgCl\downarrow$$

$$\xrightarrow[RT]{CH_2Cl_2 \text{ or } CH_2Cl_2/CS_2} Ag(P_3N_3Cl_6)_n^+[Al(OR^F)_4]^- \qquad R^F = R\ (n=2);\ R'\ (n=1) \qquad (1)$$

Similar to the synthesis of the $Ag(P_4)_n^+$ salts ($n = 1$, 2),[35,36] very small amounts of a black solid precipitated (not analyzed). Complexes **1**–**3** are stable at RT in solution and in the solid state under inert conditions. No ionization to AgCl and $P_3N_3Cl_5^+$ was observed when the solutions were exposed to ultrasound at 60 °C (12 h). The silver complexes are very soluble in CH_2Cl_2 even at low temperature. Lowering the polarity of the solution by addition of CS_2 decreased the solubility of the salts and thus facilitated crystallization. However, the presence of CS_2 influenced the constitution of the complexes present in solution: Complex **1** was obtained from $Ag[Al(OR)_4]$ and one or two equivalents of $(PNCl_2)_3$, regardless of which stoichiometry of the reagents was used, but only in a CH_2Cl_2/CS_2 solvent mixture. By contrast, complex **2** crystallized from CH_2Cl_2 at room temperature without addition of CS_2. To study the strengths of the complexation we performed a liquid- and solid-state NMR study. It has been already reported that the ^{14}N NMR resonances of $P_3N_3Cl_6$ in solution as well as the solid state are broad and hard to observe,[43] so our discussion is limited to the ^{31}P NMR results. In the ^{31}P NMR spectra the signals of complexes **1**–**3** ($\delta_{+25\,^\circ C} = 22.1$) are almost unchanged with respect to free $(PNCl_2)_3$ ($\delta_{+25\,^\circ C} = 21.7$). Lowering the temperature to −95 °C (m.p. of CH_2Cl_2) did not change the chemical shifts, and only one ^{31}P NMR resonance was observed. We failed to obtain ^{14}N NMR spectra of **1** or **2** between −95 °C and RT and with all concentrations tried.[37] The changes in the ^{31}P NMR chemical shifts on complexation are even less pronounced than those observed for the $Ag(P_4)_n^+$ ($n = 1$, 2) and $Ag(P_4S_3)_k^+$ ($k = 1$, 2, 3) complexes, in which the signals of the ligands were slightly changed by +2–10 (P_4S_3) and +25 ppm (P_4) in comparison to the free ligands. This implies that the interactions in the $Ag(P_3N_3Cl_6)_x^+$ complexes are very weak, perhaps even weaker than those in the $Ag(L)_n^+$ complexes ($L = P_4$, S_8, C_2H_2, C_2H_4, P_4S_3; $n = 1$–4).[35,36,38–42] However, in the latter set of compounds the silver atom is directly bound to the NMR-active ligand. By contrast, the interaction with the P atom in **1** and **2** is mitigated by a N atom, and therefore the influence on the chemical shift is expected to be weaker. Thus, the almost unchanged ^{31}P NMR signals of **1** and **2** may suggest: 1) Either the ^{31}P NMR shifts of all P atoms of coordinated $P_3N_3Cl_6$ are almost unchanged in comparison to the free ligand, or 2) Dynamic and exchanging species with all permutations of $Ag(CH_2Cl_2)_x(P_3N_3Cl_6)_y^+$ ($x = 0$–3, $y = 0$–2) are likely to be present in CH_2Cl_2 solution.

To illuminate this point, we optimized the structures of likely $Ag(CH_2Cl_2)_x(P_3N_3Cl_6)_y^+$ ions with $x = 0$, 1, 2 and $y = 1$, 2 with the BP86 (DFT) and MPW1PW91 (HF-DFT) functionals and calculated the chemical shifts of the phosphorus and nitrogen atoms with reference to the isolated $P_3N_3Cl_6$ molecule (Table 1).

The calculated chemical shifts for the $Ag(CH_2Cl_2)_x(P_3N_3Cl_6)_y^+$ ions in Table 1 show that the influence of the Ag^+ ion on the chemical shift of the ^{14}N and ^{31}P atoms is astonishingly small. The chemical shifts of coordinated and noncoordinated $P_3N_3Cl_6$ differ by a maximum of −1.2/+2.4 ppm (^{31}P) and +4.9 to +13.3 ppm (^{14}N), respectively.

An important question to answer now is, if there is any difference in the chemical shifts of ^{31}P and ^{14}N NMR resonances in the solid state where the complex should not be subject to dynamic of different exchanging species as suggested above and where the existence of a complex is proven by X-ray analysis (see below). Figure 1 shows ^{31}P magic angle spinning (MAS) NMR spectra of **1** recorded at different sample temperatures and different static magnetic fields. Before analyzing the spectra it is valuable to comment upon the ^{31}P MAS NMR spectrum of $P_3N_3Cl_6$, which has been studied extensively in the literature.[44] It is shown that the ^{31}P resonance is subject to residual dipolar splitting

Table 1. Computed ^{31}P and ^{14}N NMR shifts of the $Ag(CH_2Cl_2)_x(P_3N_3Cl_6)_y^+$ ions with $x=0$, 1, 2 and $y=1$, 2, referenced to the isolated $P_3N_3Cl_6$ molecule.

Compound	Atom	MPW1PW91[a]		BP86[b]	
		δ^{31}P(calcd)	δ^{14}N(calcd)	δ^{31}P(calcd)	δ^{14}N(calcd)
$P_3N_3Cl_6$		21.7[c]	106.0[c]	21.7[c]	106.0[c]
$Ag(CH_2Cl_2)(N\text{-}P_3N_3Cl_6)^+$	N1; P2,6	24.0	94.4	22.3	92.7
	N3,5; P4	22.9	100.0	21.3	101.1
$Ag(CH_2Cl_2)_2(N\text{-}P_3N_3Cl_6)^+$	N1; P2,6	24.2	97.1	23.4	96.1
	N3,5; P4	22.8	99.2	21.4	99.3
$Ag(CH_2Cl_2)(N\text{-}P_3N_3Cl_6)_2^+$	N1; P2,6	24.4	98.4	23.4	97.1
	N3,5; P4	22.8	98.1	20.5	98.2
$Ag(N\text{-}P_3N_3Cl_6)_2^+$	N1; P2,6	24.1	94.7	22.6	93.5
	N3,5; P4	22.5	95.6	20.5	97.3

[a] 6-311G(2df) basis set for C, Cl, H, P, N; SDB-cc-pVTZ basis set with 28-VE small-core ECP for Ag. [b] TZVPP basis set for C, Cl, H, P, N; TZVPPalls2 special all-electron NMR basis set for Ag (triple-zeta quality with two d and one f polarization functions). [c] Experimental[43] chemical shifts of the uncomplexed free molecules. The chemical shift calculations on $Ag(CH_2Cl_2)_x(P_3N_3Cl_6)_y^+$ were referenced to this value. The reference points for $\delta=0$ ppm are: 298.5 and 225.1 ppm (^{31}P and ^{14}N, MPW1PW91) and 262.2 and 190.2 ppm (^{31}P and ^{14}N, BP86) for the isotropic shielding tensor. Labeling of the atoms according to:

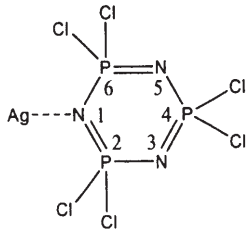

(RDS), also known as the second-order quadrupole-dipole cross term.[45] This dipolar splitting is not completely eliminated by MAS because the large quadrupolar interaction of the ^{35,37}Cl nuclei (which are directly bonded to the phosphorus atoms) tilts the axis of quantization of the ^{35,37}Cl spins away from the direction of the static magnetic field, so the angular dependence of the interaction cannot be averaged out by spinning at the magic angle. As a result ^{31}P spectra reveal complicated broadened powder patterns that change at different static magnetic fields. This broadening is more pronounced for a large quadrupolar interaction and at lower static magnetic fields. Here the appearance of RDS with the neighboring ^{14}N nuclei is neglected as it is orders of magnitude smaller.

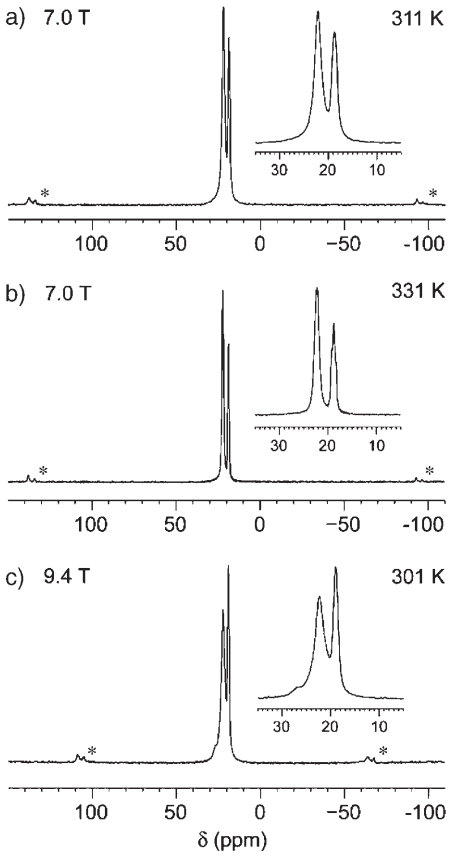

Figure 1. ^{31}P MAS NMR spectra of solid 1 recorded at the static magnetic fields of 7.0 T (a, b) and 9.4 T (c) and at the sample temperatures of a) 311 K, b) 331 K, and c) 301 K. Spinning sidebands are indicated by *. The spectra result from averaging 8 (a, b) and 64 transients (c) with a recycle interval of 600 s. No line broadening was applied.

Figure 1a shows the ^{31}P MAS NMR spectrum that appears to be constituted of two resonances with chemical shifts of $\delta=22.2$ and 18.8 ppm and with the relative intensity ratio of 2:1. In fact it is not clear at this point if these are two individual resonances or just features of a single resonance subjected to RDS due to dipole–dipole coupling with the chlorine atoms. First, it is evident that the broadening of the resonances is much smaller than in the spectrum of $P_3N_3Cl_6$ in reference [44]. This could be due to an inherently smaller quadrupolar coupling constant C_Q of ^{35,37}Cl in this complex (which is less likely), or due to motional averaging of the quadrupolar interaction. Large thermal ellipsoids for the $[Al(OR)_4]^-$ ion ligand atoms observed by X-ray diffraction suggest that the ligand is also subjected to a motional disorder. In addition, it is calculated that the barrier for the reorientation of the phosphazene rings along the N(1)–P(4) vector is associated with the fairly low-energy barrier that allows this motional reorientation to occur at the room temperature. Both, the motion of the ligand and the motion of the phosphazene ring, if they occur on the right time scale, can result in a time-dependent electric field gradient at the ^{35,37}Cl nuclei that leads to averaging of the quadrupolar interaction. An increase in the temperature is anticipated to change the motional freedom, which in turn would then result in greater averaging of the quadrupolar interaction, and subsequently lead to narrower ^{31}P resonances. This is observed in the spectrum in Figure 1b recorded at 331 K, in which two ^{31}P resonances are found to be narrower and at unchanged positions compared to the spectra in Figure 1a. This observation leads to the conclusion that these are really two individual resonances, each of which is subjected to RDS. Evidence to additionally support this conclusion is also found in the ^{31}P MAS NMR spectrum recorded at higher magnetic field (see Figure 1c), in which two resonances are observed at unchanged position but with different line broadening. The difference in line broadening of individual resonances is the result of the combined effect

of different broadening mechanisms, which are not of great importance for this study. More importantly, two ^{31}P resonances are found at the unchanged chemical shift.

The intensity ratio of the ^{31}P resonances at $\delta = 22.2$ and 18.8 ppm is 2:1 and from the crystal structure it is known that one molecule of phosphazene is contained in the asymmetric unit. Thus, we can assign the ^{31}P resonances to phosphorus sites 2,6 and 4, respectively. The small difference in ^{31}P chemical shifts predicted from the quantum-chemical calculations in Table 1 is confirmed here for the complex existing in the solid state. The changes in the chemical shift between P2,6 and P4 are so small that even very slow solution exchange processes, in which the phosphazene ligands remain coordinated to the silver ion, and which are faster than about 1 ms would lead to a collapse of the two individual resonances giving only one line in the center of mass, that is at $\delta = 21.1$ ppm in the MAS NMR experiment. Therefore one may argue that the $P_3N_3Cl_6$ ligands should remain coordinated in solution. However, exchange cannot be ruled out as the reason for the unchanged ^{31}P NMR signals of **1**–**3** (see Discussion).

Crystal structures

Compounds 1 and 2: The almost ideally D_{2h}-symmetric $Ag(P_3N_3Cl_6)_2^+$ complex in **1** consists of the Ag^+ cation centered between two coplanar $P_3N_3Cl_6$ rings (Figure 2). In **2** the silver cation is additionally coordinated by a CH_2Cl_2 molecule so that the silver atom exhibits a distorted tetrahedral coordination environment of two Cl and two N atoms (Figure 3).

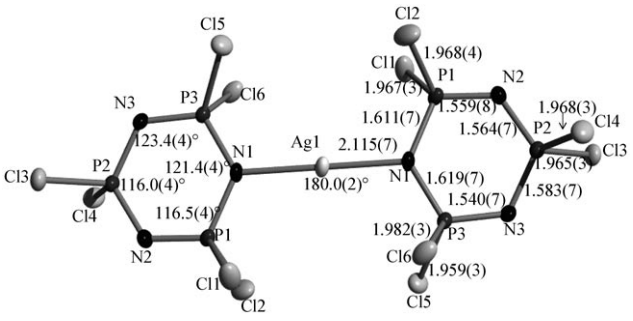

Figure 2. The planar centrosymmetric $Ag(\eta^1\text{-}P_3N_3Cl_6)_2^+$ cation in salt **1**. Thermal ellipsoids are drawn at 25% probability level.

The two phosphazene rings in **2** are twisted by about 59° with respect to each other and in comparison to the coplanar complex in **1**. The P–Cl (on average: **1** 1.969(4); **2** 1.979(1) Å) and P–N (on average: **1** 1.562(8); **2**: 1.570(2) Å) bond lengths of the phosphazene rings in **1** and **2** are comparable to those of free $P_3N_3Cl_6$ (on average: P–N 1.573; P–Cl 1.985).[46] The (Ag)N–P distances around the coordination site are elongated by about 0.042 Å (**1**) and 0.030 Å (**2**).

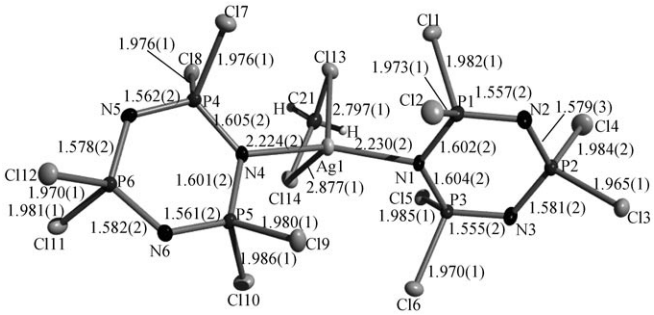

Figure 3. The almost C_2-symmetric $Ag(CH_2Cl_2)(\eta^1\text{-}P_3N_3Cl_6)_2^+$ cation in **2**. Thermal ellipsoids are drawn at 25% probability level.

The dative Ag–N bonds are about 0.11 Å shorter and therefore stronger in **1** (2.115(7) Å) than in **2** (2.227(2) Å). The average Ag–Cl distance in **2** (2.837 Å) is slightly longer than that in the $Ag(CH_2Cl_2)_3^+$ complex (2.752 Å).[39] These trends were also confirmed by ab initio calculations (see Table 1). However, the differences between the calculated and experimental Ag–N and $Ag^+\cdots Cl(CH_2Cl_2)$ distances of −0.108 Å and +0.137 Å are larger than the usual discrepancy between experiment and theory of 0.03 to 0.05 Å. The reason for this discrepancy is attributed to the weak bonds and hence the shallow potential-energy wells of the calculation. The interactions of the chlorine atoms of the hexachlorotriphosphazene ligand and the silver cation are insignificant, since all Ag–Cl contacts are longer than the sum of the van der Waals radii of Cl and Ag (3.5 Å).

The cations in **1** and **2** are isolated molecular ions with only minor interactions with the $[Al(OR)_4]^-$ anions. Complex **1** forms a distorted CsCl structure, and complex **2** a distorted NaCl structure.[47] The fluorine contacts to the cations are weak and only approach the chlorine atoms, apart from two very weak contacts to the silver cation (see Supporting Information).

Compound 3: The complex consists of a $P_3N_3Cl_6$ ring coordinated through an N atom to the silver cation (Figure 4). Since the $[Al(OC(CH_3)(CF_3)_2)_4]^-$ ion is more strongly coordinating than $[Al(OC(CF_3)_3]^-$, the Ag^+ ion exhibits two stronger Ag–O contacts at 2.442(3) Å and 2.345(4) Å (av 2.394(4) Å), on average slightly longer than those in $Ag(CH_2Cl_2)[Al(OR')_4]$[34] (Ag–O 2.377(5) and 2.386(4) Å, av 2.382(5) Å).

The dative Ag–N bond (2.227(4) Å) is longer than that in **1** (2.115(7) Å) but similar to that in **2** (av 2.227(2) Å). The similarity of these Ag–N distances in **2** and **3** suggests that one CH_2Cl_2 and one $(PNCl_2)_3$ molecule in **2** are similar donors towards the Ag^+ ion as the two oxygen atoms of the OR′ groups in **3**. The P–N and P–Cl distances are comparable with those in the $(PNCl_2)_3$ rings in **2** (see Table 2). The (Ag)N1–P bonds of, on average, 1.604(5) Å are elongated by 0.03 Å in comparison to the free ligand. The silver cation is eight-coordinate and exhibits, apart from the Ag–O and Ag–N interactions, five Ag–F contacts, three of which are

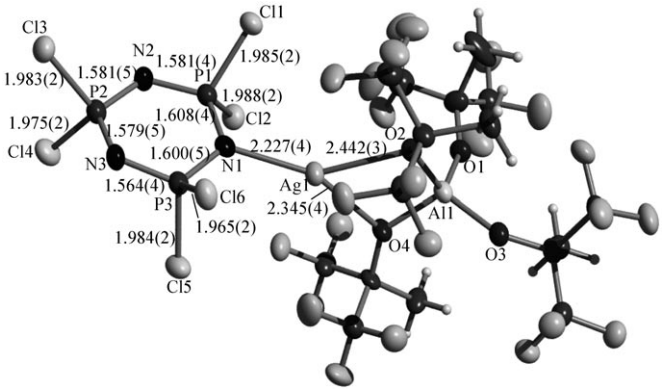

Figure 4. Section of the solid-state structure of **3**. Thermal ellipsoids are drawn at 25 % probability level.

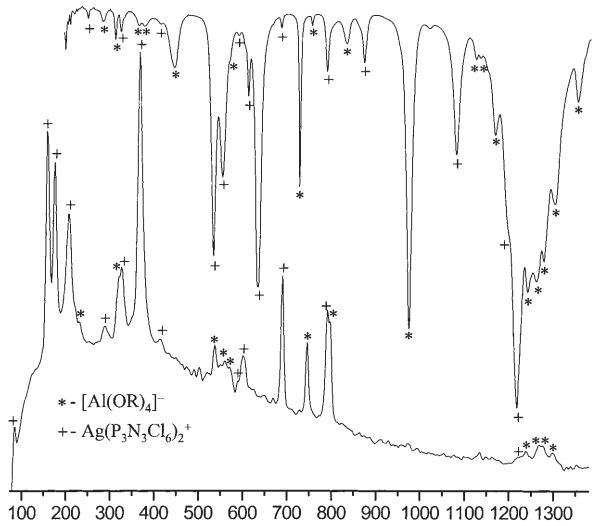

Figure 5. Overlay of the FTIR (top) and FT Raman (bottom) spectra of **1**.

stronger (2.815, 2.880, and 2.894 Å) and two weaker (3.057 and 3.108 Å).[48]

Vibrational spectroscopy: The IR spectra of **1** and **3** and a low-temperature Raman spectrum of **1** were recorded (Figure 5); crystals of **3** gave no Raman spectrum. Based on the IR and Raman spectra of free $(PNCl_2)_3$[17,18,20] and frequency calculations on $Ag(P_3N_3Cl_6)_2^+$, $Ag(P_3N_3Cl_6)^+$, and $P_3N_3Cl_6$ at the BP86/SVP level, we tentatively assigned the vibrations of each complex (Table 3).

The spectra of **1** and **3** (Supporting Information, Figure M), apart from the anion vibrations, are similar to the spectrum of free $(PNCl_2)_3$, but some bands split due to the reduction of the local symmetry on coordination. The almost unchanged frequencies of the coordinated versus free phosphazene molecules further underline the weak coordination that is only stable in the presence of a very weakly coordinating anion. All observed and calculated vibrations are listed in Table 3 and are grouped with the calculated frequencies so that similar vibrations in **1** (IR and Raman), **3** (IR), and free $(PNCl_2)_3$ (IR and Raman) are in the same row. For a more detailed discussion, see the Supporting Information.

Discussion

Considering that several studies on the preparation of hexahalotriphosphazene complexes have appeared,[7,8,24–26,28–30,52] it is astonishing that the solid-state X-ray structure of any type of adduct of $(PNX_2)_3$ (X = halogen) was hitherto unknown. The crystal structures of **1**–**3** clearly assign the preferred phosphazene coordination site versus Ag^+ to the nitrogen atoms.

Experimental silver ion affinity (SIA): In earlier investigations we assessed the SIA of several ligands towards the silver ion. Based on experimental results, we established a comparative scale of the donor strengths of the ligands $C_6H_5CH_3$ (Tol), 1,2-dichloroethane, CH_2Cl_2, P_4S_3, S_8, and

Table 2. Important experimental and calculated bond lengths of the silver-coordinated phosphazene rings in complexes **1**–**3**.

Distance	**1**	**1** (MP2[a])	**2** (av)	**2** (MP2[a])	$P_3N_3Cl_6$	$P_3N_3Cl_6$ (MP2[a])	**3**	**3** (MP2[a])
Ag1–N1	2.115(7)	2.070	2.227(2)	2.118			2.227(4)	2.120
P1–N1	1.611(7)	1.635	1.602(2)	1.627			1.608(4)	1.634
P3–N1	1.619(7)	1.635	1.605(2)	1.630			1.600(5)	1.634
P3–N3	1.540(7)	1.572	1.559(2)	1.574			1.564(4)	1.569
P1–N2	1.559(8)	1.572	1.559(2)	1.574			1.581(4)	1.569
P2–N3	1.583(7)	1.601	1.581(2)	1.600	1.573	1.595	1.579(5)	1.603
P2–N2	1.564(7)	1.601	1.579(2)	1.600			1.581(5)	1.603
P–Cl′	1.959(3)–1.982(3)	1.996 av	1.970(1)–1.986(1)	1.999 av			1.965(2)–1.988(2)	1.995
	1.969(4) av		1.979(1) av				1.981(2) av	
P–Cl″	1.967(3) av	1.984 av	1.965(1)–1.984(2)	1.985 av	1.983–1.988	2.006	1.979(2) av	1.979
			1.975(2) av					
Ag···Cl(P)	3.640–3.688	3.663–3.670	3.509–3.939	3.569–3.958			3.638–3.854	3.693
	3.662 av	3.667 av	3.735 av	3.708 av			3.758 av	
Ag–Cl(C)			2.837(1)[b]	2.974				

[a] TZVPP basis set. [b] Compare to the six Ag–Cl distances in $Ag(CH_2Cl_2)_3^+[(RO)_3AlFAl(OR)_3]^-$ of 2.661(2) to 2.836(2), av 2.752(2) Å.[39]

Table 3. Experimental and calculated IR and Raman (RA) vibrations of **1** and **3**.

1 IR	**1** calcd and assignment ν [km mol^{-1}][c]	**1** RA	$(PNCl_2)_3$ exptl ν (int. [%])	$(PNCl_2)_3$ calcd[c] ν [km mol^{-1}]	IR[a] $[Al(OR)_4]^-$	**3** IR	**3** calcd/assignment	IR[b] $[Al(OR')_4]^-$
	63(0) δ_{op}(ring)	86(10)[d]	RA: 59(25)	32(0)				
	158(0) PCl_2 rocking	160(75)	RA: 163(45)	157(0)				
	185(0) δ_{op}(ring)	176(60)	RA: 179(45)	185(0)				
	200(0) PCl_2 wagging	207(40)	IR: 208(vw)	199(4)				
			RA: 206(40)					
213(vw)	$[Al(OR)_4]^-$				IR: 215(w)			
					RA: 216(5)			
	221(0) PCl_2 twisting		IR: 220(w)	199(4)				
			RA: 220(5)					
252(vw)	237(14) PCl_2 bending							
	$[Al(OR)_4]^-$	232(5)			RA: 232(5)			
					RA: 245(5)			
287(w)	$[Al(OR)_4]^-$				284(w)			
	287(0) (N-PCl_2-N) rocking	290(5)				328(w)	$[Al(OR')_4]^-$	328(w)
314(w)	$[Al(OR)_4]^-$				314(w)			
327(w)	296(10) (Cl_2P-N_2) rocking	329(20)	IR: 335(w)	305(5)				
			RA: 338(20)					
332(w)	$[Al(OR)_4]^-$	321(sh)			RA: 318(sh)			
					IR: 330(vw)			
367(w)	$[Al(OR)_4]^-$				367(w)	336(w)	$[Al(OR')_4]^-$	338(w)
	334(10); 335(0) $\nu_s(PCl_2)$	367(100)	RA: 364(100)	330(0)		371(w)	335(7)	
380(w)	$[Al(OR)_4]^-$				377(w)	385(sh)	$[Al(OR')_4]^-$	385(w)
417(w)	IR: 356(6) RA: 351(0)	414(3)	IR: 404(vw)	346(1)		398(m)	351(7)	
	δ_{op}(ring)		RA: 406(5)					
446(m)	$[Al(OR)_4]^-$				445(m)	439(w)	$[Al(OR')_4]^-$	434(w)
						456(w)	$[Al(OR')_4]^-$	455(vw)
536(s)	503(384) δ_{ip}(ring)		IR: 528(s)	504(298)		528(s)	498(218)	
	$[Al(OR)_4]^-$	537(10)			RA: 537(38)	544(m)	528(240)	
555(s)	526(614) δ_{ip}(ring)		IR: 550(sh)			554(m)	?	
	$[Al(OR)_4]^-$	560(5)			RA: 562(24)			
	$[Al(OR)_4]^-$	570(5)			RA: 572(18)	569(m)	$[Al(OR')_4]^-$	565(w)
571(w)	$[Al(OR)_4]^-$				571(w)			
590(vw)	560(0) $\nu_{as}(PCl_2)$	590(sh)	IR: 583(w)					
	608(0) δ_{op}(ring)	601(10)	RA: 578(15), 597(5)	555(0)				
612(m)	581(48) δ_{op}(ring)					612(vs)	580(90)	
						626(sh)	$[Al(OR')_4]^-$	622(w)
635(vs)	614(828) δ_{op}(ring)		IR: 612(vs)	593(524)		633(m)	616(392)	
689(w)	IR: 639(6) RA: 642(0)	689(40)	IR: 670(vw)	616(0)				
	N-P-N bending		RA: 667(70)					
728(s)	$[Al(OR)_4]^-$				728(s)	702(m)	$[Al(OR')_4]^-$	701(m)
	$[Al(OR)_4]^-$	745(25)			RA: 745(20)	735(w)	$[Al(OR')_4]^-$	724(m), 737(m)
755(w)	$[Al(OR)_4]^-$				755(w)	772(w)	$[Al(OR')_4]^-$	773(sh)
789(m)	IR: 745(186)	791(30)	IR: 783(vw)	754(0)				
	RA: 749(0)		RA: 783(40)					
	ring breathing mode							
						780(sh)	$[Al(OR')_4]^-$	780(w)
	$[Al(OR)_4]^-$	795(30)			RA: 797(20)	796(m)	$[Al(OR')_4]^-$	793(w)
832(w)	$[Al(OR)_4]^-$				832(m)	818(sh)	$[Al(OR')_4]^-$	817(sh)
859(sh)	836(52) ν_s(P-N_{Ag}-P)			838(1)		846(w)	829(3)	
872(m)	841(5) (PN_2) twisting		IR: 874(w)	838(1)				
			RA: 875(1)					
						866(w)	$[Al(OR')_4]^-$	866(w)
974(vs)	$[Al(OR)_4]^-$				973(vs)	978(w)	$[Al(OR')_4]^-$	979(sh)
						991(w)	$[Al(OR')_4]^-$	992(w)
						1002(w)	$[Al(OR')_4]^-$	1004(w)
						1014(w)	$[Al(OR')_4]^-$	
1080(s)	1005(680) ν_{as}(P-N_{Ag}-P)					1083(s)	985(435)	
1123(w)	$[Al(OR)_4]^-$					1087(s)	$[Al(OR')_4]^-$	1087(vs)
1133(w)	$[Al(OR)_4]^-$				1133(sh)	1115(s)	$[Al(OR')_4]^-$	1114(s)
1168(m)	$[Al(OR)_4]^-$				1169(ms)	1141(sh)	$[Al(OR')_4]^-$	
1192(sh)	1176(954) $\nu_{as}(PN_2)$		IR: 1197(s)	1176(1034)		1197(s)	1176(507)	
			RA: 1221(1)					
1218(vs)	IR: 1232(2705)	1218(5)	IR: 1217(vs)	1176(1034)		1218(vs)	1244(1129)	
	RA: 1241(0),							
	$\nu_s(PN_2)$							

Table 3. (Continued)

1 IR	**1** calcd and assignment ν [km mol^{-1}][c]	**1** RA	$(PNCl_2)_3$ exptl ν (int. [%])	$(PNCl_2)_3$ calcd[c] ν [km mol^{-1}]	IR[a] $[Al(OR)_4]^-$	**3** IR	**3** calcd/assignment	IR[b] $[Al(OR')_4]^-$
1242(s)	$[Al(OR)_4]^-$	1239(5)			1242(vs)	1241(s)	$[Al(OR')_4]^-$	1243(s)
			IR: 1251(m)			1258(s)	$[Al(OR')_4]^-$	–
			RA: 1251(25)					
1261(s)	$[Al(OR)_4]^-$	1268(10)			1264(s)	1311(m)	$[Al(OR')_4]^-$	1310(m)
1277(s)	$[Al(OR)_4]^-$	1274(10)			1276(vs)			
1301(s)	$[Al(OR)_4]^-$	1297(5)			1301(s)			
			IR: 1314(w)					

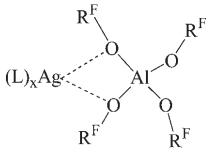

Figure 6. Silver coordination in the Lewis acid–base complexes $(L)_xAgAl(OR^F)_4$ ($x=1$, 2; $R^F=C(H)(CF_3)_2$, $C(CH_3)(CF_3)_2$).

P_4.[42] The structural basis for this assessment is shown in Figure 6. An ordering according to the average Ag–O bond lengths would imply a linear relation between the bond energy and the bond lengths. However, it is known that the relation between bond energy and bond lengths is better described by an exponential decrease of the bond energy with increasing bond length, as included in I. D. Brown's bond-valence method.[42] Thus, the SIA is the sum of the bond valences (in v.u.) of the two Ag–O contacts, as in Figure 6. The higher the SIA value, the stronger the interaction between the silver ion and the oxygen atoms of the anion, but the weaker the interaction of the ligand L with the silver ion (Table 4).[42]

Table 4. Ag–O bond valences s [v.u.] and SIA of several Lewis acid–base complexes.[a]

Complex[a]	s		$\Sigma(s)$ = SIA	Ref.
$(Tol)_2Ag[Al(OR'')_4]$	0.119	0.118	0.236	[42]
$(C_2H_4Cl_2)_2Ag[Al(OR'')_4]$	0.160	0.126	0.286	[42]
$(S_8)Ag[Al(OR'')_4]$	0.252	0.080	0.332	[42]
$(P_4S_3)Ag[Al(OR'')_4]$	0.190	0.170	0.370	[42]
$(P_3N_3Cl_6)Ag[Al(OR')_4]$	0.186	0.252	0.438	this work
$(CH_2Cl_2)Ag[Al(OR')_4]$	0.228	0.221	0.449	[42]
$(P_4)Ag[Al(OR')_4]$	0.236	0.220	0.456	[42]

[a] $R'=C(CH_3)(CF_3)_2$; $R''=C(H)(CF_3)_2$.

According to its SIA value (0.438), $P_3N_3Cl_6$ is a rather weak ligand for Ag^+, a bit better than CH_2Cl_2 (0.449 v.u.) or P_4 (0.456 v.u.), but much weaker than S_8 (0.332 v.u.) or toluene (0.236 v.u.). This finding is also in agreement with the average Ag–Cl distance in **2**, which is 0.089 Å longer than that in the homoleptic $Ag(CH_2Cl_2)_3^+$ ion. Thus $(PNCl_2)_3$ is a slightly stronger ligand than CH_2Cl_2.

Dynamics of the $Ag^+/P_3N_3Cl_6/CH_2Cl_2$ mixture: Since we could only present indirect evidence for the presence of $Ag(P_3N_3Cl_6)_x^+$ complexes in solution, we analyzed the system with further lattice-energy and Born–Haber cycle calculations to establish the quality of the ab initio energetics. Thus, by using the calculated[53–55] lattice potential enthalpies of the salts and the published sublimation/evaporation enthalpy of $P_3N_3Cl_6$[56]/CH_2Cl_2[57] in a deposited Born–Haber cycle (BHC), $\Delta_rH(g)$ for the formation of $Ag(P_3N_3Cl_6)_2(CH_2Cl_2)^+_{(g)}$ from $Ag(CH_2Cl_2)_3^+{}_{(g)}$ and $2\,P_3N_3Cl_{6(g)}$ was estimated to be less than -126 kJ mol^{-1} [cf. Eq. (2h) in Table 5]. This BHC-derived upper limit of -126 kJ mol^{-1} is in excellent agreement with the MP2 calculated value of -126.1 kJ mol^{-1} and thereby supports the validity of the quantum-chemical MP2 calculations.

We now turn to a detailed analysis of the dynamics in CH_2Cl_2 solution [Eqs. (2a)–(2i) in Table 5]. All calculations were done at the MP2/TZVPP level with inclusion of zero-point energies and entropic, thermal, and solvation contributions at 298 K (COSMO in CH_2Cl_2). For comparison the BP86 and MPW1PW91 results are also included.

Comparison to the BHC data for Equation (2h) ($\Delta_rH \leq -126$ kJ mol^{-1}) suggests that the DFT (-51 kJ mol^{-1}) and HF-DFT (-58 kJ mol^{-1}) calculations underestimate the Ag–N bond enthalpies. In contrast to the MP2 calculations (Δ_rH[Eq. (2h)] = -126 kJ mol^{-1}), the DFT and HF-DFT calculations do not account for dispersive interactions and therefore likely give consistently lower complexation energies. However, the latter calculations also suggest that $P_3N_3Cl_6$ should be bound to Ag^+ in solution with the two major players being $Ag(P_3N_3Cl_6)_2^+$ and $Ag(CH_2Cl_2)(P_3N_3Cl_6)_2^+$. With the DFT and HF-DFT calculations, exchange according to Equations (2e), (2f), (2i) is likely, while MP2 indicates that exchange should only occur for the CH_2Cl_2 molecule [Eq. (2f)], but likely not for the phosphazene ligands [Eqs. (2e) and (2i)].[58]

Ground state of complex 1: The D_{2h}-symmetric structure of **1** found in the solid state is a transition state in the gas phase (one imaginary frequency at $3i$ cm^{-1}). A D_2-symmetric structure in which the two phosphazene rings are twisted by about 54.4° was calculated to be the ground state (see Figure 7); $\Delta H_{(g)}$ for such a transformation amounts to only $+1$ kJ mol^{-1}.

Thus, in the solid state this distortion can easily be induced by packing effects. A similar situation was observed

Table 5. Thermodynamic data of the dynamics of the $Ag^+/P_3N_3Cl_6/CH_2Cl_2$ mixture in the gas phase and solution (COSMO model, $\varepsilon_r = 8.93$) calculated with ab initio and hybrid HF-DFT methods. Values in bold indicate the three most likely exchange reactions at the respective level.

Reaction (L = $P_3N_3Cl_6$, D = CH_2Cl_2)	Equation	(RI-)MP2/TZVPP			(RI-)BP86/SVP			MPW1PW91[a]		
		$\Delta H_{(g)}$	$\Delta G^{\circ}_{(g)}$	$\Delta G^{\circ}_{CH_2Cl_2}$	$\Delta H_{(g)}$	$\Delta G^{\circ}_{(g)}$	$\Delta G^{\circ}_{CH_2Cl_2}$	$\Delta H_{(g)}$	$\Delta G^{\circ}_{(g)}$	$\Delta G^{\circ}_{CH_2Cl_2}$
$Ag(D)_3^+ + L \rightleftarrows Ag(D)_2L^+ + D$	(2a)	−61	−46	−31	−27	−13	+4	−31	−16	+1
$Ag(D)_2L^+ \rightleftarrows Ag(L)_2D^+ + D$	(2b)	−66	−88	−77	−24	−47	−34	−28	−51	−38
$Ag(D)_2L^+ \rightleftarrows Ag(D)L^+ + D$	(2c)	56	9	−10	+50	+2	−16	33	−15	−33
$2\,Ag(D)_2L^+ \rightleftarrows Ag(L)_2D^+ + Ag(D)_3^+$	(2d)	−5	−42	−46	+3	−34	−38	+3	−34	−39
$Ag(D)L^+ + L \rightleftarrows Ag(L)_2D^+$	(2e)	−122	−97	**−67**	−74	−49	**−18**	−61	−36	**−5**
$Ag(L)_2D^+ \rightleftarrows Ag(L)_2^+ + D$	(2f)	+46	+19	**+11**	+21	−8	**−15**	16	−13	**−20**
$Ag(D)_3^+ + 2L \rightleftarrows Ag(L)_2^+ + 3D$	(2g)	−79	−115	−97	−31	−68	−45	−43	−79	−57
$Ag(D)_3^+ + 2L \rightleftarrows Ag(L)_2D^+ + 2D$	(2h)	−126	−134	−107	−51	−59	−30	−59	−67	−37
$AgLD^+ + L \rightleftarrows Ag(L)_2^+ + D$	(2i)	−75	−78	**−57**	−53	−57	**−33**	−45	−48	**−24**

[a] 6-311G(2df) basis set except for Ag, for which a SDB-cc-pVTZ basis with relativistically adjusted 28 VE effective-core potential was used.

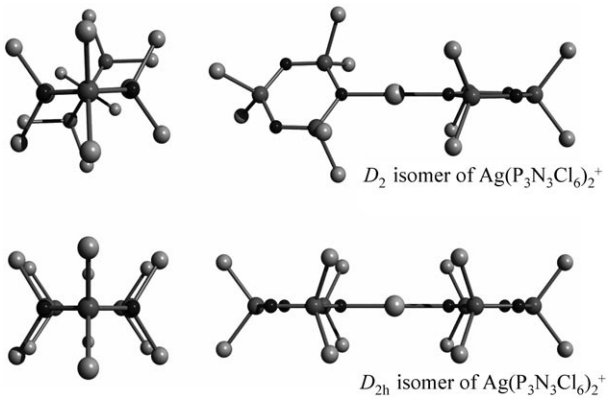

Figure 7. Calculated D_2- and D_{2h}-symmetric structures of $Ag(P_3N_3Cl_6)_2^+$ (MP2/TZVPP).

for the ground-state structure of the $Ag(P_4)_2^+$ complex: The experimental structure[35,36,38] is dependent on temperature and counterion. Weak solid-state contacts to the fluorine atoms of the anion distort the almost D_{2h}-symmetric structure with $[Al(OR)_4]^-$ from that calculated to be the global minimum in the gas phase (D_2).[39,59] We suppose that a similar situation occurs in the solid-state structure of **1**. In the calculated D_{2h}-symmetric $Ag(N\text{-}P_3N_3Cl_6)_2^+$ structure the shortest Cl···Cl contact was found to be 4.424 Å, and that in the D_2 structure 5.142 Å, that is, a slight weakening of the Cl···Cl Coulombic repulsion may be the reason for the lowering of the gas-phase symmetry from D_{2h} to D_2.

Other $Ag(P_3N_3Cl_6)_x^+$ isomers: The linear twofold coordination in complex **1** is typical for the Ag^+ ion and observed in many $Ag(L)_2^+$ complexes with soft ligands.[52] However, we also calculated other possible coordination modes for complexes **1** and **3**, that is, coordination through the Cl atoms. Ag···Cl coordination represents the HOMO–LUMO interaction (the HOMO of $P_3N_3Cl_6$ is Cl-centered). η^2-*Cl*,*Cl* and η^3-*Cl*,*Cl*,*Cl* interactions were assessed (see Table 6 and Figure 8 and Supporting Information). Similar and isostructural coordination elements ($Ag\cdots Cl_2E$) were found within the $Ag(CH_2Cl_2)_3^+$ complex (E = CH_2).[39]

The formation of complexes with Cl coordination is unfavorable by 37–140 kJ mol^{-1} ($\Delta G^{\circ}_{CH_2Cl_2}$). The next most favorable structure is a $Ag(\eta^3\text{-}Cl,Cl,Cl\text{-}P_3N_3Cl_6)^+$ isomer with η^3 coordination of three Cl atoms (Figure 8). This isomer,

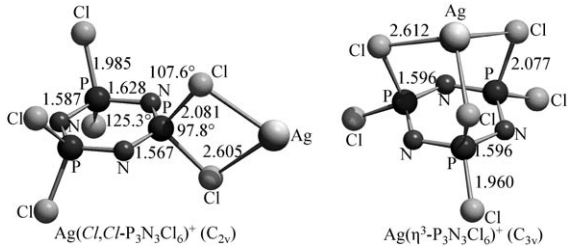

Figure 8. Examples for other coordination modes of Ag^+–($P_3N_3Cl_6$) complexes: $Ag(\eta^2\text{-}Cl,Cl\text{-}P_3N_3Cl_6)$ (C_{2v}) and $Ag(\eta^3\text{-}Cl,Cl,Cl\text{-}P_3N_3Cl_6)$ (C_{3v}) at the MP2/TZVPP level.

calculated to be a true minimum in this conformation, is unfavorable by +27 to +37 kJ mol^{-1} with respect to $Ag(N\text{-}P_3N_3Cl_6)^+$. These low-lying higher energy isomers may also serve as an additional pathway in the possible exchange of the $Ag(CH_2Cl_2)_x(P_3N_3Cl_6)_y^+$ ions in solution.[60]

On the existence of the $P_3N_3Cl_5^+$ ion: Since the $Ag^+/P_3N_3Cl_6$ mixture is stable at room temperature in solution, and even treatment at about 50–60 °C in an ultrasonic bath did not lead to ionization of the P–Cl bond, we were interested whether the $P_3N_3Cl_5^+$ cation could be obtained on the basis of the underlying thermodynamics and whether the

Table 6. $\Delta H_{(g)}$, $\Delta G^{\circ}_{(g)}$, $\Delta G^{\circ}_{CH_2Cl_2}$ for the isomerization of the silver hexachlorotriphosphazene complexes.

Isomerization	$\Delta H_{(g)}$	$\Delta G^{\circ}_{(g)}$	$\Delta G^{\circ}_{CH_2Cl_2}$
$Ag(N\text{-}P_3N_3Cl_6)^+ \rightarrow Ag(\eta^2\text{-}Cl,Cl\text{-}P_3N_3Cl_6)^+$	+70	+61	+51
$Ag(N\text{-}P_3N_3Cl_6)^+ \rightarrow Ag(\eta^3\text{-}Cl,Cl,Cl\text{-}P_3N_3Cl_6)^+$	+27	+27	+37
$Ag(N\text{-}P_3N_3Cl_6)_2^+ \rightarrow Ag(\eta^2\text{-}Cl,Cl\text{-}P_3N_3Cl_6)(N\text{-}P_3N_3Cl_6)^+$	+85	+77	+71
$Ag(\eta^2\text{-}Cl,Cl\text{-}P_3N_3Cl_6)(N\text{-}P_3N_3Cl_6)^+ \rightarrow Ag(\eta^2\text{-}Cl,Cl\text{-}P_3N_3Cl_6)_2^+$	+73	+80	+69
$Ag(N\text{-}P_3N_3Cl_6)_2^+ \rightarrow Ag(\eta^3\text{-}Cl,Cl,Cl\text{-}P_3N_3Cl_6)(N\text{-}P_3N_3Cl_6)^+$	+58	+47	+45

stability of the complexes is only kinetic (Only the most accurate MP2 calculations were used). According to the calculated energetics in Table 5, the true "starting material" should be the (exchanging?) complex cation in **1** (or **2**). We calculated the Gibbs reaction energy for formation of the $P_3N_3Cl_5^+$ cation via the likely $Ag(N\text{-}P_3N_3Cl_6)(\eta^3\text{-}Cl,Cl,Cl\text{-}P_3N_3Cl_6)^+$ intermediate. This lowest energy species with a direct Ag–Cl bond must be reached prior to ionization of the P–Cl bond with formation of $P_3N_3Cl_5^+$ and AgCl (Figure 9).

The reaction starting from complex **1** has a barrier of at least $+226\,kJ\,mol^{-1}$ for the ionization ($45+181\,kJ\,mol^{-1}$). Thus, although the entire reaction is exergonic by $5\,kJ\,mol^{-1}$ ($226–231=-5\,kJ\,mol^{-1}$), the silver salt clearly is not a suitable agent to generate the $P_3N_3Cl_5^+$ cation. However, $\Delta G^{o}_{CH_2Cl_2}$ for the formation of the $P_3N_3X_5^+$ cations (X = Br, I) from $Ag(CH_2Cl_2)_3^+$ and $(PNX_2)_3$ is more favorable by up to $80\,kJ\,mol^{-1}$ than that of $P_3N_3Cl_5^+$ and may therefore proceed (see Supporting Information).

Figure 9 shows that to obtain the $P_3N_3Cl_5^+$ cation, an ionizing agent is required that will *not* preferably form a complex and which reacts at low temperatures. A likely candidate would be $AsBr_4^+[Al(OR)_4]^-$, which we have shown to react with CS_2 to give $CS_2Br_3^+$.[61] Since the ionization energies—as a measure of the HOMO energies—of CS_2 (10.08 eV)[62] and $(PNCl_2)_3$ (10.05 eV)[63] are very similar, the use of $AsBr_4^+$ as an ionizing agent is promising (e.g., $AsBr_4^+ + P_3N_3X_3 \rightarrow P_3N_3X_5^+ + BrX + AsBr_3$).

Conclusion and Outlook

The first complexes of any hexahalophosphazene molecule that were characterized by their crystal structure have been presented, that is, $Ag(P_3N_3Cl_6)_2^+$, $Ag(CH_2Cl_2)(P_3N_3Cl_6)_2^+$, and $Ag(P_3N_3Cl_6)^+$, stabilized in the environment of weakly coordinating $[Al(OR^F)_4]^-$ ions. N-coordinated structures of coordinated hexachlorotriphosphazene were found and also calculated to be the most favorable; an $\eta^3\text{-}Cl,Cl,Cl\text{-}P_3N_3Cl_6$ complex is the next most accessible isomer.

According to the SIA scale of $Ag(L)^+$ complexes (L = ligand) with ligands like P_4, S_8, CH_2Cl_2, and $P_3N_3Cl_6$, the donor strength of $P_3N_3Cl_6$ is much lower than that of S_8 but comparable to that of a very weak base like P_4 or CH_2Cl_2. In agreement with this, the competitive coordination of CH_2Cl_2 and $(PNCl_2)_3$ was observed. MAS ^{31}P NMR spectra clearly proved that the chemical shift of the P atoms in $P_3N_3Cl_6$ is almost unchanged upon complexation, and $\Delta\delta(^{31}P)$ is as small as 2 ppm. This conclusion is further underlined by quantum-chemical calculations of the chemical shifts of several $Ag(P_3N_3Cl_6)_x(CH_2Cl_2)_y^+$ isomers and highlights the weak coordination of the $P_3N_3Cl_6$ ligand. Therefore, weakly coordinating anions were necessary to stabilize these complexes.

The formation of $P_3N_3Cl_5^+$ was never observed, even at $+60\,°C$ in an ultrasonic bath. Accordingly, we calculated the minimum barrier for $P_3N_3Cl_5^+$ formation from $Ag(P_3N_3Cl_6)_2^+$ to be $+226\,kJ\,mol^{-1}$. Other reagents to which the phosphazene does not coordinate as a ligand are likely better suited to achieve this goal, for example, $AsBr_4^+$.

Experimental Section

General: All manipulations were performed using standard Schlenk or dry box techniques and a dinitrogen or argon atmosphere (<1 ppm H_2O and O_2). Apparatus was closed by J. Young valves with a glass stem (leaktight at −80 °C). All solvents were rigorously dried over P_2O_5 and degassed prior to use and stored under N_2. $P_3N_3Cl_6$ was purchased from Merck KGaA and stored under inert atmosphere. $Ag[Al(OR)_4]$[34] and $Ag[Al(OR')_4]$[34] were prepared according to the literature. Raman and IR spectra were recorded using a 1064 nm laser on a Bruker IFS 66v spectrometer equipped with the Raman module FRA106. IR spectra were recorded on Nujol mulls between CsI plates. NMR spectra of sealed samples were run on a Bruker AC250 spectrometer in CD_2Cl_2 and were referenced to the solvent (^1H, ^{13}C) or external H_3PO_4 (^{31}P) and aqueous $AlCl_3$ (^{27}Al).

NMR spectroscopy: Liquid-state NMR spectra of samples dissolved in CD_2Cl_2 and packed in sealed NMR tubes were recorded on a Bruker AC250 spectrometer equipped with a 5.9 T narrow bore magnet. The ^1H and ^{13}C chemical shifts are reported in ppm relative to an internal standard of TMS, while the ^{27}Al and ^{31}P chemical shifts are reported in ppm relative to an external standard of 1 M $Al(NO_3)_3$(aq) and 85 % H_3PO_4(aq), respectively.

Solid-state NMR spectra were recorded on a Bruker DRX 300 and Avance 400 NMR spectrometers equipped with 7.0 and 9.4 T widebore magnets, respectively, and utilizing 4-mm CPMAS and 2.5-mm CPMAS probeheads, respectively. Nicely powdered samples are packed under an N_2 atmosphere into 4-mm and 2.5-mm outer diameter ZrO_2 rotors and the magic angle sample spinning was used at the rate of 14 kHz. The sample temperature was calibrated by using $Pb(NO_3)_2$

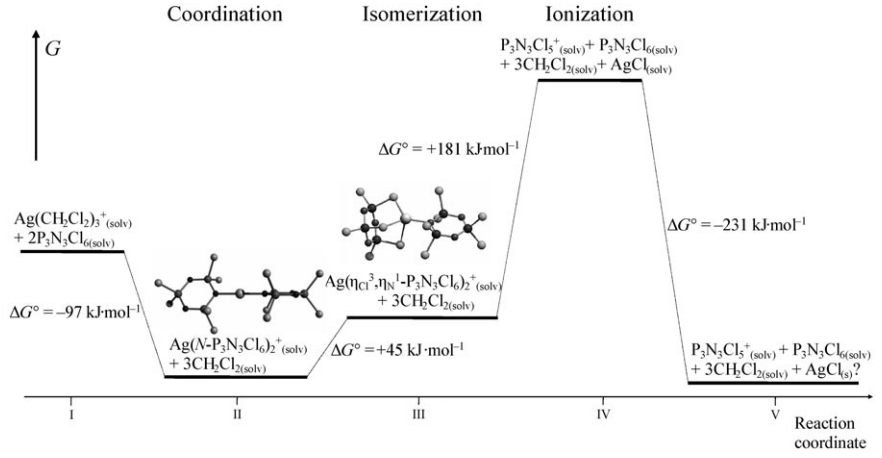

Figure 9. Calculated 298 K Gibbs energies in CH_2Cl_2 solution for the reaction between $Ag(CH_2Cl_2)_3^+$ and $2\,P_3N_3Cl_6$ leading to $P_3N_3Cl_5^+$ (MP2/TZVPP).

under spinning conditions, while the absolute temperature was calculated from the chemical shift difference of the two proton resonances in liquid methanol.[64] Chemical shifts of ^{31}P are reported in ppm relative to an external 85% H_3PO_4(aq) standard.

Synthesis of $Ag(P_3N_3Cl_6)_2^+[Al(OR)_4]^-$ (R=C(CF$_3$)$_3$)

Stoichiometry 1:1: $(CH_2Cl_2)Ag[Al(OR)_4]$ (1.453 g, 1.253 mmol) and $(PNCl_2)_3$ (0.436 g, 1.253 mmol) were loaded into a two-bulbed vessel closed by Young valves. The solids were dissolved in CH_2Cl_2 (10 mL) at −78 °C. The solution immediately became slightly dark and an opalescent suspension formed. The flask was left at −80 °C overnight. Only small quantities of a fine brown to nearly black precipitate were formed. The flask was stored at −30 °C (1 d) and finally at ambient temperature (three days), but no solid AgCl was formed. The solution was filtered and CS_2 (3 mL) was added to the solution. Colorless plate-shaped single crystals of **1** were obtained at −80 °C over one week (yield 0.859 g, 74% based on $(PNCl_2)_3$).

^{31}P NMR (101 MHz, CD_2Cl_2, −40 °C): $\delta = 22.1$ ppm (s, $\nu_{1/2} = 169$ Hz); ^{13}C NMR (63 MHz, CD_2Cl_2, +25 °C): $\delta = 120.7$ ppm (q, $J_{C,F} = 291.5$ Hz, CF_3, anion); ^{27}Al NMR (78 MHz, CD_2Cl_2, +25 °C): $\delta = 37.6$ ppm (s, $\nu_{1/2} = 45.5$ Hz).

Stoichiometry 1:2: $(CH_2Cl_2)Ag[Al(OR)_4]$ (1.473 g, 1.270 mmol) and $(PNCl_2)_3$ (0.884 g, 2.540 mmol) were loaded into a two-bulbed vessel closed by Young valves. The solids were dissolved in CH_2Cl_2 (10 mL) and CS_2 (3 mL) at ambient temperature. The solution immediately became slightly dark and an opalescent suspension formed. The mixture was left for 30 min, during which time a colorless solution over a fine nearly black precipitate formed. The solution was filtered, concentrated to about one-half, and crystallized. Colorless plate-shaped single crystals were obtained at −80 °C (yield 2.020 g of crystals, 86%). Analytical data were as above.

Synthesis of $Ag(CH_2Cl_2)(P_3N_3Cl_6)_2^+[Al(OR)_4]^-$ (R=C(CF$_3$)$_3$): $Ag[Al(OR)_4]$ (0.830 g, 0.716 mmol) and $(PNCl_2)_3$ (0.498 g, 1.430 mmol) were loaded into a two-bulbed vessel closed by Young valves. The solids were dissolved in CH_2Cl_2 (10 mL) at ambient temperature. The solution immediately became slightly dark and an opalescent suspension formed. The mixture was left for about 15 min, after which time a colorless solution over a fine, nearly black precipitate formed. The solution was filtered and concentrated to about one-half. No crystals were obtained at −28 °C, and the reaction mixture was further slowly concentrated at room temperature to an oily residue, from which colorless plate-shaped single crystals of **2** were grown. After selection of a suitable crystal of **2** for X-ray diffraction, the crystals (yield 1.050 g, 83%) were isolated by decantation and pumped dry under dynamic vacuum until the weight of the flask was constant (coordinated CH_2Cl_2 was removed). The NMR spectra were identical with that of **1**. IR and Raman (low-temperature) spectra were recorded (see Vibrational Spectroscopy section).

Synthesis of $Ag(P_3N_3Cl_6)^+[Al(OR')_4]^-$ (R′=C(CH$_3$)(CF$_3$)$_2$): $(CH_2Cl_2)Ag[Al(OR')_4]$ (0.841 g, 0.709 mmol) and $(PNCl_2)_3$ (0.247 g, 0.709 mmol) were loaded into a two-bulbed vessel closed by Young valves. The solids were dissolved in CH_2Cl_2 (15 mL) and CS_2 (3 mL) at ambient temperature. The solution immediately became slightly dark and an opalescent suspension formed. The mixture was left for two days at ambient temperature, after which time a colorless solution over a fine brown to nearly black precipitate formed. The solution was filtered, concentrated to about one-half, and left for crystallization at −28 °C. After 2 d single crystals had grown as very fine colorless plates (yield 0.750 g, 77%).

^{31}P NMR (101 MHz, CD_2Cl_2, +25 °C): $\delta = 22.1$ ppm (s, $\nu_{1/2} = 160.6$ Hz); ^{13}C NMR (63 MHz, CD_2Cl_2, +25 °C): $\delta = 124.2$ (q, $J_{C,F} = 288.3$ Hz, CF_3), 76.2 (septet), $J_{C,F} = 29.8$ Hz, $C(CF_3)_2$), 18.0 ppm (s, CH_3); ^{19}F NMR (235 MHz, +25 °C): $\delta = -79.2$ ppm (s); ^{27}Al NMR (78 MHz, CD_2Cl_2, +25 °C): $\delta = 48.0$ ppm (s, $\nu_{1/2} = 370.5$ Hz).

X-ray crystal structure determination: Data for X-ray structure determinations were collected on a STOE IPDS II diffractometer using graphite-monochromated $Mo_{K\alpha}$ radiation (0.71073 Å). Single crystals were mounted in perfluoroether oil on top of a glass fiber and then brought into the cold stream of a low-temperature device so that the oil solidified. All calculations were performed on PCs using the SHELX97 software package. The structures were solved by direct methods and successive interpretation of the difference Fourier maps, followed by least-squares refinement (see Table 7). Due to disorder of the $[Al(OR)_4]^-$ ion in **1** the refinement of the structure only converged at $R1 = 0.0937$. Several data sets of different batches and at different temperatures showed that this disorder is inherent to all crystals of **1**. However, only the structural parameters of the anion are afflicted by the disorder. The cation is well behaved, as judged by comparison to the calculated data and the thermal ellipsoid plot. All CF_3 groups in the asymmetric unit of **1** had to be split over two positions, and the disordered atoms were included in the refinement anisotropically to give occupations of about 25% for the disordered atoms (see Supporting Information). The positions of all CF_3 groups were fixed with SADI, DFIX, and DANG restraints. The four C atoms of one of the $C(CF_3)_3$ groups in the anion of **2** had to be split over two positions giving an occupation number of 20% for the disordered atoms (all atoms were refined anisotropically). The hydrogen atoms of the CH_3 groups in the anion of **3** were included in the refinement in calculated positions by a riding model using fixed isotropic parameters. All other atoms in **3** were refined anisotropically. CCDC-259935, CCDC-259936, and CCDC-259934 contain the supplementary crystallographic data for this paper. These data can be obtained free of charge from the Cambridge Crystallographic Data Centre via www.ccdc.cam.ac.uk/data_request/cif.

Table 7. Crystallographic details for $Ag(P_3N_3Cl_6)_2^+[Al(OR)_4]^-$ (**1**), $(CH_2Cl_2)Ag(P_3N_3Cl_6)_2^+[Al(OR)_4]^-$ (**2**), and $Ag(P_3N_3Cl_6)^+[Al(OR'')_4]^-$ (**3**) (R = C(CF$_3$)$_3$, R″ = C(CH$_3$)(CF$_3$)$_2$).

	1	**2**	**3**
crystal size [mm]	0.15×0.2×0.25	0.8×0.6×0.5	1.0×1.4×0.2
crystal system	monoclinic	orthorhombic	monoclinic
space group	*C*2/*c*	$P2_12_12_1$	$P2_1/c$
a [Å]	17.536(4)	16.904(3)	20.889(4)
b [Å]	15.877(3)	17.099(3)	10.396(2)
c [Å]	19.606(4)	20.057(3)	20.566(4)
α [°]	90.000	90	90
β [°]	105.79(3)	90	117.53(3)
γ [°]	90.000	90	90
volume [Å^3]	5252.8(18)	5797.3(2)	3960.3(2)
Z	4	4	4
ρ_{calcd} [Mg m^{-3}]	2.239	2.223	2.088
μ [mm^{-1}]	1.361	1.422	1.257
max./min. trans.	0.8485/0.9157	0.3002/0.4274	0.7071/0.9269
index range	$-19 \le h \le 19$	$-21 \le h \le 21$	$-22 \le h \le 22$
	$-17 \le k \le 17$	$-21 \le k \le 21$	$-11 \le k \le 10$
	$-21 \le l \le 21$	$-25 \le l \le 24$	$-20 \le l \le 20$
completeness (%)/ 2θ [°]	97.2/46.5	99.3/54.2	92.4/45.2
temp, [K]	120	120	120
refl. collected	15516	45988	18097
refl. unique	3664	12676	4842
refl. observed (2σ)	2639	12255	3849
R (int.)	0.0805	0.0867	0.1328
GOOF/GOOF restrained	1.039/1.030	1.037/1.037	1.046/1.046
final *R*/*wR*2 (2σ)	0.0937/0.2465	0.0377/0.0932	0.0746/0.1925
final *R*/*wR*2 (all data)	0.1228/0.2708	0.0392/0.0946	0.0859/0.2052
larg. res. peak [e Å^3]	0.466	0.960	1.086

Computational details: Most computations were done with the program TURBOMOLE.[65] The geometries of all species were optimized at the (RI-)MP2 level[66] with triple-ζ valence polarization (two d and one f functions) TZVPP basis set.[67,68] The 28- and 46-electron cores of Ag and I were replaced by a quasirelativistic effective core potential.[69] All species were also fully optimized at the BP86/SV(P) DFT level.[70–74] Approximate solvation energies (CH_2Cl_2 solution with $\varepsilon_r = 8.93$) were calculated with the COSMO model[72] at the BP86/SV(P) DFT level using the MP2/TZVPP geometries. Frequency calculations were performed for all species and structures, which represent true minima without imaginary frequencies on the respective hypersurface if not explicitly stated other-

wise. For thermodynamic calculations the zero-point energy and thermal contributions to the enthalpy and the free energy at 298 K were included. The thermal contributions to the enthalpy and entropic contributions to the free energy were calculated with the program FreeH included in TURBOMOLE. NMR shifts at the BP86/TZVPP level (Ag: TZVPPalls2 all-electron basis set optimized for NMR calculations) were calculated as single points on the BP86/SVP optimized geometries. The MPW1PW91/6-311G(2df) calculations (Ag: SDB-cc-pVTZ valence basis with 28 VE small-core ECP) were done with Gaussian 03, and NMR shifts were computed from fully optimized structures obtained at the same level.[76] The MPW1PW91/6-311G(2df) level was selected, since it also reproduced quantum-chemical problem cases such as the S_4^{2+} and S_8^{2+} ions,[77–80] as well as giving reliable ^{31}P chemical shifts and P,P coupling constants of ternary PSX cations (X = Br, I).[80] All calculated chemical shifts are deposited together with machine-readable *xyz* orientations of the calculated structures and the calculated vibrational frequencies in the Supporting Information.

Acknowledgements

This work was supported by the Deutsche Forschungsgemeinschaft, the Fonds der Chemischen Industrie, the Universität Karlsruhe (TH), and the EPF Lausanne. We are grateful to Prof. H. Schnöckel for many useful discussions as well as to Dr. Sawatzki from the Bruker Optics demonstration lab in Ettlingen, Germany, for recording the low-temperature Raman spectrum of **1**, which otherwise always decomposed in the laser beam.

[1] V. Chandrasekhar, K. R. J. Thomas, *Struct. Bonding (Berlin)* **1993**, *81*, 41–113.
[2] H. R. Allcock, F. W. Lampe, J. E. Mark, *Contemporary Polymer Chemistry*, Pearson Prentice Hall, Upper Saddle River, NJ, **2003**.
[3] R. A. Shaw, B. W. Fitzsimmons, B. C. Smith, *Chem. Rev.* **1962**, *62*, 247–281.
[4] J. C. Van de Grampel, *Rev. Inorg. Chem.* **1981**, *3*, 1–28.
[5] J. E. Mark, H. R. Allcock, R. West, *Inorganic Polymers*, Prentice Hall, Englewood Cliffs, NJ, **1992**.
[6] A. Chandrasekaran, S. S. Krishnamurthy, M. Nethaji, *Inorg. Chem.* **1994**, *33*, 3085–3090.
[7] H. R. Allcock, L. J. Wagner, M. L. Levin, *J. Am. Chem. Soc.* **1983**, *105*, 1321–1327.
[8] H. R. Allcock, G. H. Riding, R. R. Whittle, *J. Am. Chem. Soc.* **1984**, *106*, 5561–5567.
[9] R. J. Waltman, B. Lengsfield, J. Pacansky, *Chem. Mater.* **1997**, *9*, 2185–2196.
[10] H. Sasaki, M. Shoji, T. Nakakawaji, M. Ishida, Y. Ito, H. Ishihara (Hitachi Ltd., Japan), JP-A 99-374799 and JP-A 2001187796, **2001**.
[11] R. Jaeger, M. Debowski, I. Manners, G. J. Vancso, *Inorg. Chem.* **1999**, *38*, 1153–1159.
[12] H. Sabzyan, Z. Kalantar, *THEOCHEM* **2003**, *663*, 149–157.
[13] K. F. Ferris, P. Friedman, D. M. Friedrich, *International Journal of Quantum Chemistry, Int. J. Quantum Chem. Symp.* **1988**, *22*, 207–218.
[14] J. B. Lagowski, R. Jaeger, I. Manners, G. J. Vancso, *Polym. Prepr. Am. Chem. Soc. Div. Polym. Chem.* **1993**, *34*, 326–327.
[15] S. S. Krishnamurthy, *Phosphorus Sulfur Silicon Relat. Elem.* **1994**, *87*, 101–111.
[16] K. F. Ferris, C. B. Duke, *International Journal of Quantum Chemistry, Int. J. Quantum Chem. Symp.* **1989**, *23*, 397–407.
[17] P. C. Painter, J. Zarian, M. M. Coleman, *Appl. Spectrosc.* **1982**, *36*, 265–271.
[18] J. P. Huvenne, G. Vergoten, P. Legrand, *J. Mol. Struct.* **1980**, *63*, 47–57.
[19] D. M. Adams, A. C. Shaw, *Spectrochim. Acta Part A* **1991**, *47*, 1551–1557.
[20] J. Weidlein, E. Schmid, E. Fluck, *Z. Anorg. Allg. Chem.* **1976**, *420*, 280–284.
[21] H. Sun, P. Ren, J. R. Fried, *Comput. Theor. Polym. Sci.* **1998**, *8*, 229–246.
[22] M. Breza, *THEOCHEM* **1998**, *454*, 77–81.
[23] B. Lakatos, A. Hesz, Z. Vetessy, G. Horvath, *Acta Chim. Acad. Sci. Hung.* **1969**, *60*, 309–331.
[24] G. E. Coxon, D. B. Sowerby, *J. Chem. Soc. A* **1969**, 3012–3014.
[25] T. Chivers, N. L. Paddock, *J. Chem. Soc. A* **1969**, 1687–1689.
[26] H. Binder, *Z. Anorg. Allg. Chem.* **1971**, *383*, 130–135.
[27] M. F. Lappert, G. Srivastava, *J. Chem. Soc. A* **1966**, 210–211.
[28] N. K. Hota, R. O. Harris, *J. Chem. Soc. Chem. Commun.* **1972**, 407–408.
[29] B. P. Baranwal, S. S. Das, U. Farva, *Research* **2001**, *5*, 55–58.
[30] F. Kandemirli, *Phosphorus Sulfur Silicon Relat. Elem.* **2003**, *178*, 2331–2342.
[31] I. Manners, *Angew. Chem.* **1996**, *108*, 1712–1731; *Angew. Chem. Int. Ed. Engl.* **1996**, *35*, 1602–1621.
[32] S. Pohl, O. Petersen, H. W. Roesky, *Chem. Ber.* **1979**, *112*, 1545–1549.
[33] M. N. Nobis, A. R. McWilliams, O. Nuyken, I. Manners, *Macromolecules* **2000**, *33*, 7707–7712.
[34] I. Krossing, *Chem. Eur. J.* **2001**, *7*, 490–502.
[35] I. Krossing, *J. Am. Chem. Soc.* **2001**, *123*, 4603–4604.
[36] I. Krossing, L. Van Wüllen, *Chem. Eur. J.* **2002**, *8*, 700–711.
[37] However, we succeeded in observing the ^{14}N NMR signal of pure $P_3N_3Cl_6$ in CD_2Cl_2 solution.
[38] I. Krossing, I. Raabe, *Angew. Chem.* **2004**, *116*, 2116–2142; *Angew. Chem. Int. Ed.* **2004**, *43*, 2066–2090.
[39] A. Bihlmeier, M. Gonsior, I. Raabe, N. Trapp, I. Krossing, *Chem. Eur. J.* **2004**, *10*, 5041–5051.
[40] I. Krossing, A. Reisinger, *Angew. Chem.* **2003**, *115*, 5903–5906; *Angew. Chem. Int. Ed.* **2003**, *42*, 5725–5728.
[41] T. S. Cameron, A. Decken, I. Dionne, M. Fang, I. Krossing, J. Passmore, *Chem. Eur. J.* **2002**, *8*, 3386–3401.
[42] A. Adolf, M. Gonsior, I. Krossing, *J. Am. Chem. Soc.* **2002**, *124*, 7111–7116.
[43] J. Mason, W. van Bronswijk, J. G. Vinter, *J. Chem. Soc. Dalton Trans.* **1977**, 2337–2339.
[44] a) S. Paasch, K. Krueger, B. Thomas, *Solid State Nucl. Magn. Reson.* **1995**, *4*, 267; b) B. Thomas, S. Paasch, S. Steuernagel, K. Eichele, *Solid State Nucl. Magn. Reson.* **2001**, *20*, 108.
[45] a) J. G. Hexem, M. H. Frey, S. J. Opella, *J. Am. Chem. Soc.* **1981**, *103*, 224; b) A. Naito, S. Ganapathy, C. A. McDowell, *J. Chem. Phys.* **1981**, *74*, 5393; c) R. K. Harris, A. C. Olivieri, *Prog. NMR Spectrosc.* **1992**, *24*, 435; d) C. A. McDowell in *Encyclopedia of Nuclear Magnetic Resonance, Vol. 5* (Eds.: D. M. Grant, R. K. Harris), Wiley, Chichester, **1996**, p. 2901.
[46] G. J. Bullen, *J. Chem. Soc. B* **1971**, 1450.
[47] This packing follows the expectations based on the simple radius-ratio rules of the solid-state structure adopted; that is, the smaller cation in **1** resides in the larger cubic interstice of the CsCl structure, and the larger cation in **2** in the smaller octahedral interstice of the NaCl structure (see Supporting Information).
[48] Sum of the van der Waals radii of Ag and O: 3.10 Å; Ag and N: 3.20 Å; Ag and F: 3.20 Å; see Supporting Information.
[49] I. Krossing, I. Raabe, *Angew. Chem.* **2001**, *113*, 4544–4547; *Angew. Chem. Int. Ed.* **2001**, *40*, 4406–4409.
[50] M. Gonsior, I. Krossing, L. Müller, I. Raabe, M. Jansen, L. Van Wüllen, *Chem. Eur. J.* **2002**, *8*, 4475–4492.
[51] I. Krossing, A. Reisinger, unpublished results.
[52] P. Schwerdfeger, P. D. W. Boyd, A. K. Burrell, W. T. Robinson, M. Taylor, *Inorg. Chem.* **1990**, *29*, 3593.
[53] H. D. B. Jenkins, H. K. Roobottom, J. Passmore, L. Glasser, *Inorg. Chem.* **1999**, *38*, 3609–3620.
[54] H. K. Roobottom, H. D. B. Jenkins, J. Passmore, L. Glasser, *J. Chem. Educ.* **1999**, *76*, 1570–1573.
[55] H. D. B. Jenkins, H. K. Roobottom, J. Passmore, *Inorg. Chem.* **2003**, *42*, 2886–2893.

[56] R. Steinman, F. B. Schirmer Jr., L. F. Audrieth, *J. Am. Chem. Soc.* **1942**, *64*, 2377–2378.
[57] NIST Chemistry webbook.
[58] Since $P_3N_3Cl_6$ has three independent nitrogen binding sites, exchange may also take place by an associative mechanism involving a bridging phosphazene ligand. However, due to the size of the species involved, it was not attempted to model this exchange by quantum chemistry.
[59] H.-C. Tai, I. Krossing, M. Seth, D. V. Deubel, *Organometallics* **2004**, *23*, 2343–2349.
[60] All other isomers that were assessed but are not included in Table 6 or Figure 9 were not true minima or relaxed on lowering the symmetry to a structure in which Ag^+ coordinates to the N atom.
[61] M. Gonsior, I. Krossing, *Chem. Eur. J.* **2004**, *10*, 5730–5736.
[62] L. Wang, J. E. Reutt, Y. T. Lee, D. A. Shirley, *J. Electron Spectrosc. Relat. Phenom.* **1988**, *47*, 167.
[63] P. Clare, D. B. Sowerby, *J. Inorg. Nucl. Chem.* **1981**, *43*, 477.
[64] a) P. A. Beckmann, C. Dybowski, *J. Magn. Reson.* **2000**, *146*, 379; b) A. L. van Geet, *Anal. Chem.* **1970**, *42*, 679.
[65] R. Ahlrichs, M. Bär, M. Häser, H. Horn, C. Kölmel, *Chem. Phys. Lett.* **1989**, *162*, 165.
[66] F. Weigend, M. Häser, *Theor. Chim. Acta* **1997**, *97*, 331.
[67] A. Schäfer, H. Horn, R. Ahlrichs, *J. Chem. Phys.* **1992**, *97*, 2571.
[68] A. Schäfer, C. Huber, R. Ahlrichs, *J. Chem. Phys.* **1994**, *100*, 5829.
[69] W. Kuechle, M. Dolg, H. Stoll, H. Preuss, *Mol. Phys.* **1991**, *74*, 1245.
[70] J. C. Slater, *Phys. Rev.* **1951**, *81*, 385–390.
[71] S. H. Vosko, L. Wilk, M. Nusair, *Can. J. Phys.* **1980**, *58*, 1200–1211.
[72] A. D. Becke, *Phys. Rev. A* **1988**, *38*, 3098–3100.
[73] J. P. Perdew, *Phys. Rev. B* **1986**, *33*, 8822.
[74] K. Eichkorn, O. Treutler, H. Oehm, M. Häser, R. Ahlrichs, *Chem. Phys. Lett.* **1995**, *242*, 652–660.
[75] A. Klamt, G. Schürmann, *J. Chem. Soc. Perkin Trans. 1* **1993**, *2*, 799.
[76] Gaussian 03, Version 6.0, Gaussian Inc., Pittsburg PA, **2003**.
[77] T. S. Cameron, R. J. Deeth, I. Dionne, H. Du, H. D. B. Jenkins, I. Krossing, J. Passmore, H. K. Roobottom, *Inorg. Chem.* **2000**, *39*, 5614–5631.
[78] H. D. B. Jenkins, L. C. Jitariu, I. Krossing, J. Passmore, R. Suontamo, *J. Comput. Chem.* **2000**, *21*, 218–226.
[79] I. Krossing, J. Passmore, *Inorg. Chem.* **1999**, *38*, 5203–5211.
[80] M. Gonsior, I. Krossing, E. Matern, *Chem. Eur. J.* **2005**, accepted, DOI: 10.1002/chem.200500138.

Received: March 2, 2005
Revised: September 5, 2005
Published online: December 23, 2005

